

DOI: 10.5862/JPM.253.9

UDC: 53.07

*V.B. Bondarenko, S.N. Davydov, P.G. Gabdullin
N.M. Gnuchev, A.V. Maslevtsov, A.A. Arkhipov*

Peter the Great St. Petersburg Polytechnic University

ELECTRON SPECTROMETER FOR STUDYING FIELD-INDUCED EMISSION FROM NANOSTRUCTURED OBJECTS

A novel electron spectrometer has been designed to study low-voltage field-induced emission of nanostructures such as nanoporous carbon, nanotubes, nanodiamond and other carbon structures. The estimated high resolving power of the device is mainly achieved by using an original energy analyser of high energy dispersion and by retarding the electron beam by the factor of tens and hundreds in terms of energy. The analyser pass energy governs the absolute energy resolution ΔE of the spectrometer; ΔE value varies approximately in the range of $10 \text{ meV} < \Delta E < 300 \text{ meV}$. There are three different working modes adapted for emission of widely variable current. The minimal emission current at which energy analysis is still possible is approximately 0.1 nA . The spectrometer working modes were tested experimentally using a thermoemitter as the test object. The study then proved that the recorded spectra reflected physical phenomena taking place on the emitter surface.

LOW-VOLTAGE FIELD EMISSION, NANOSTRUCTURE, HIGH RESOLUTION, ELECTRON SPECTROMETER.

Introduction

Nowadays, a lot of materials are known which are formed from structural elements measured in nanometers and tens of nanometers. These are so-called nanoporous carbons [1, 2], carbon nanotubes [3], nanodiamond and nanocarbon films [4], nanodiamond composites [5], graphene films [6].

A distinctive property of these nanostructured materials is their capability to emit electrons at rather low strength of the electrostatic field (around 1 kV/mm) which is $10^3 - 10^4$ times less than the values typical for cold field emission of metals. Even though this phenomenon has been investigated for many years, the question of its physical nature has not yet been fully answered.

The analysis of the energy spectra of emitted electrons could have been one of the natural methods for studying this low-voltage field-induced emission. The idea of separating a flow of charged particles into monokinetic components is not in itself original, but for the field emission, even in the case of low-voltage one, such separation meets some specific troubles.

This work presents a description and experimental test results for a novel spectrometer, which has been elaborated and made especially to record electron field emission spectra.

The ways to increase the spectrometer resolving power

The spectrometer consists of an electrostatic analyzer 1, receiving zoom lens 2 and electron collector 3 (Fig. 1, a). The lens input diaphragm 'looks' at the surface of the sample 4 under study. The initial part of the electron way from the sample (emitter) to the collector lies inside the lens. The resolving power of the analyzer proper is

$$R_a = \frac{E_p}{\Delta E} = D \frac{X}{\Delta x_1 + \Delta x_2 + \xi}, \quad (1)$$

where E_p is the analyzer pass energy (the energy of the electron entering the analyzer input diaphragm); ΔE is the absolute energy resolution (in eV); X is the representative size of the device (here it is the distance between the input and output diaphragm centers: $X = x_2 - x_1$); D is the analyzer energy dispersion expressed in the units of X (reduced dispersion):

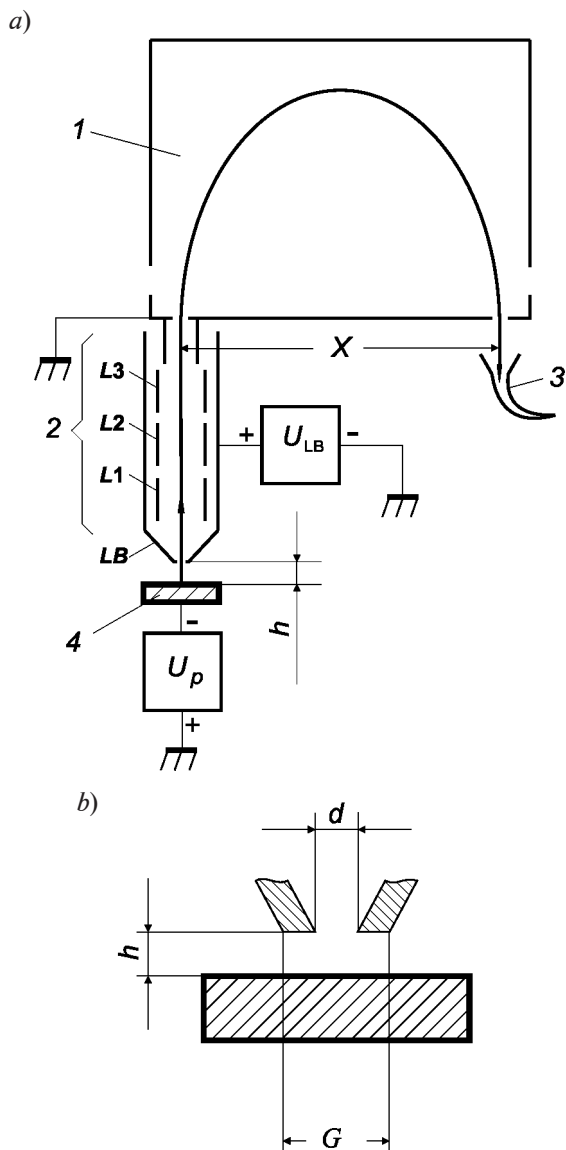


Fig. 1. The scheme of the spectrometer (a) and magnified positions 4, 2 (in part) with geometric parameters (b):

1 - energy analyser; 2 - retarding lens; 3 - electron collector; 4 - sample (emitter); LB - lens body; L_i - focusing electrodes; U_p , U_{LB} - power supply of potentials

$$D = \frac{E_p}{X} \cdot \frac{dx}{dE};$$

Δx_1 and Δx_2 are the input and output diaphragm widths respectively; ξ is the measure of the aberration blurring of the input diaphragm image in the vicinity of the output diaphragm.

Let both diaphragms be at zero potential

(see Fig. 1, a), and the emitter under investigation be at the potential $U_p = -|E_p / e|$, where e is the electron charge.

Then, in the vicinity of the sample surface, the strength of the electric field "pulling" electrons out is

$$F = \frac{U_{LB} - U_p}{h},$$

Where h is the vacuum gap between the lens entrance aperture and the emitter surface (see also Fig. 1, b); U_{LB} is the positive potential applied to the lens electrode with the entrance aperture. Electrons entering this aperture possess kinetic energy

$$|(U_{LB} - U_p) \cdot e|.$$

For some reasons (for instance, because of the emitter roughness or the entrance aperture finiteness), the value h cannot be made too small, and on average $h \approx 0.5 - 1.0$ mm. As a result, the emission threshold potential

$$U_{LB} - U_p \approx 500 - 1000 \text{ V}.$$

Consequently, the minimal energy of electrons at the entrance aperture of the lens (and, actually, of the whole spectrometer) should be approximately equal to 500 eV. On the other hand, the resolution needed in the experiment is about $kT = 25$ meV, that is the electron thermal energy spread at room temperature (here k is the Boltzmann constant, T is the emitter temperature). So, the minimal value of the resolving power of the spectrometer should be rather high:

$$R_{sp \min} \approx 500 \cdot 10^3 \text{ mV} / 25 \text{ mV} = 2 \cdot 10^4.$$

R_{sp} can be enlarged by several methods, though each of them has some weaknesses:

(i) The analyzer size X can be increased (see Eq. (1)). Increasing X makes the spectrometer more expensive. Moreover, it demands stronger vacuum pumping and more careful protection of the spectrometer from any stray fields including the Earth's magnetic field.

(ii) The analyzer diaphragm sizes Δx_1 and Δx_2 can be decreased. This will inevitably cause reduction of the recorded signal intensity, apart from the fact that it will be impossible to produce the spectrometer in case of excessive diaphragm decrease.

(iii) It is possible to try to diminish beam divergence at the analyzer entrance $2\Delta\alpha$. This will bring ξ closer to zero but, of course, the signal intensity will be decreased.

(iv) Since, according to Eq. (1), ΔE is proportional to E_p , the beam deceleration in the lens makes R_{sp} bigger. The electron energy

$$E = |(U_{LB} - U_p) e|$$

at the lens entrance and the corresponding F value can be kept invariable by increasing U_{LB} . Unfortunately, if the lens magnification factor is equal to unity, then, according to the Helmholtz – Lagrange law, the beam divergence at the analyzer entrance is increased by a factor of $\sqrt{E / E_p}$.

All of these methods were used somehow when the spectrometer was being designed. There could have been one extra way to increase R_{sp} : it is increasing the reduced dispersion D of the analyzer. But this parameter is an inherent characteristic of the electrostatic field which separates monokinetic components of the beam. It is well known [7] that the D value varies in a very narrow range ($0.8 < D < 1.2$) under the focusing conditions in the fields of simple geometry (plane, spherical, cylindrical).

Energy analyzer of increased dispersion

In Refs. [8–12], a construction, principle of operation and experimental tests of a non-traditional energy analyzer were described. The device is based on a two-dimensional electrostatic field with the plane of symmetry (yz):

$$U(x, y) = \frac{\text{sh}^2 2\pi y - \sin^2 2\pi x}{(\text{ch} 2\pi y + \cos 2\pi x)^2}. \quad (2)$$

Expression (2) is written in a specific system of units where the energy unit is the analyzer pass energy E_p , the potential unit is $|E_p / e|$ and the length one is the distance X between the point source and its point image. The solution of Eq. (2) with respect to y gives us the following equipotentials:

$$y = \text{arcch}[U \cos 2\pi x + [1 + (1 - 2U) \sin^2 2\pi x]^{1/2} \cdot (1 - U)^{-1}] \cdot (2\pi)^{-1}.$$

The (xy)-plane cross-sections of some of these equipotentials are shown in Fig. 2, *a*.

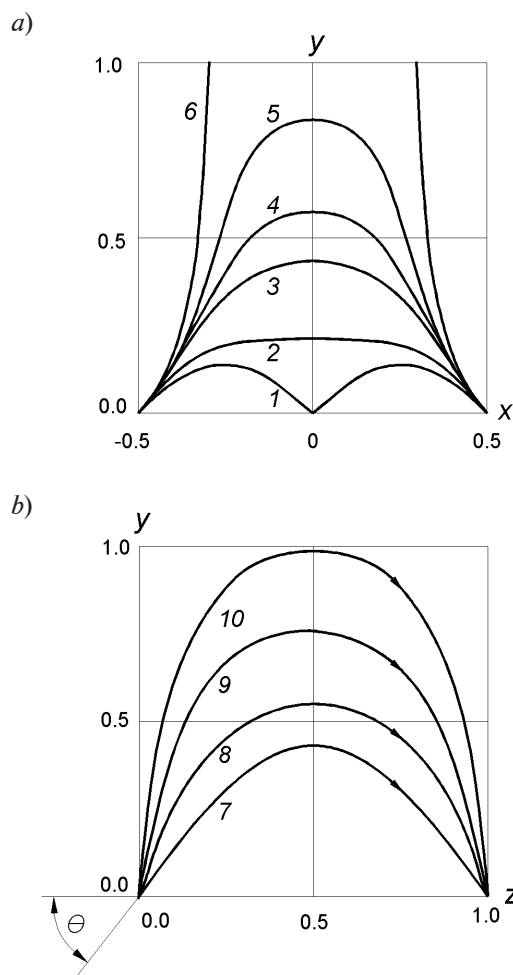


Fig. 2. (xy)-Cross-section of some equipotentials of electrostatic field with (yz)-plane of symmetry (*a*) and trajectories of the electrons entering the field in the (yz)-plane at different polar angles θ (*b*). *a* – potential U , a.u.: 0 (1), 0.300 (2), 0.700 (3), 0.900 (4), 0.975 (5), 1.000 (6); *b* – angle θ , degrees: 57 (7), 70 (8), 80 (9), 85 (10). Focusing in (yz)-plane is perfect

In the plane of symmetry, the field possesses ideal focusing: an electron, moving in the plane (yz) and starting its flight from the origin with the unit initial energy E_p at any polar angle with respect to the z axis, will definitely come to the point ($x = 1, y = 0, z = 0$). Some trajectories of this kind are shown in Fig. 2, *b*.

In the same plane, the reduced dispersion

$$D = \frac{1}{2 \cos^2 \theta}. \quad (3)$$

It is seen from Eq. (3) that D grows with θ , and when θ approaches $\pi/2$, D tends to infinity.

From this point of view, it is reasonable to design the analyzer with the maximal value of the entrance polar angle θ . But the height of the trajectory increases with θ (see Fig. 2, *b*), and this fact implies the increase in the size of the device. Moreover, the electron kinetic energy at the top part of the trajectory decreases with θ growth, and this circumstance again demands more careful protection of the spectrometer from any stray fields including the Earth's magnetic field. Furthermore, to enhance the optical efficiency of the analyzer, the working mode for the device should be chosen so that focusing exists not only in the (yz) -plane but in the x -direction as well, in other words, the spatial focusing exists. Calculations have shown [13] that from this point of view, the $\theta \approx 80^\circ$ regime is optimal at which little focusing appears in the x -direction, the source image becomes most compact, and $D \approx 16.6$, which is more than ten times more than the typical dispersion of any simple field structures.

In reality, though, the electrode shapes are slightly different from the ideal ones because the last are difficult to be produced. As a consequence, the reduced dispersion, which actually depends on the working mode, is a bit smaller: $D \approx 12 - 13$. The device has been made from copper, its base dimension $X = 50$ mm, it measures $65 \times 70 \times 80$ mm. It is provided with changeable diaphragms from 0.2 to 0.6 mm in width.

Retarding system

After choosing the field structure of the high-dispersion analyzer, the next step towards enhancing the spectrometer resolving power is creating a lens (retarding system) which will decelerate the electron beam, before it enters the volume of the analyzer, from the extraction energy E (as it was mentioned, $E \approx 1$ keV or higher) to E_p .

A five-electrode axisymmetric lens 2 (see Fig. 1, *a*) was designed and made. The inner diameter of the focusing electrodes is 8 mm, the whole length of the system is 36 mm. To extract electrons from the emitter 4, the lens body is fed with positive voltage U_{LB} . Then, along their trajectories, electrons are consequently influenced by the focusing electrode potentials $L1$, $L2$, and $L3$. The last, fifth, electrode is me-

chanically and electrically joined to the lower electrode of the analyzer, their common potential being zero. Taking into consideration the feed circuit described, the lens electron energy retarding coefficient is

$$K_{dec} = \frac{|U_{LB}| + |U_p|}{|U_p|} = \frac{U_{LB} - U_p}{|U_p|}. \quad (4)$$

Transportation and focusing electrons are deeply influenced by the potential pattern near the emitter surface. In Fig. 3, it is shown how the potential picture of the electron trajectories alters with the distance h (see also Fig. 1, *b*) between the sample surface and the lens end. The calculations were done using 'Simion 7' software. The lens entrance diaphragm diameter d was taken to be equal to 0.4 mm, the outer diameter of the lens body end $G = 1.0$ mm. Fig. 3 also shows the trajectories of the electrons starting their flights from the emitter surface at right angle to it.

Electrons start their movement from the emitter surface along the normal with the initial energy of 20 meV. The potential relief between the surface and lens butt is shown as an equidistant equipotential series. The equipotentials are practically horizontal near the emitter surface (on the bottom) and are essentially curved in the vicinity of the butt. In all the three patterns, the first particle moves along the axis of symmetry, while the subsequent electrons start their flights with the step $\Delta r = 30 \mu\text{m}$ along the radial coordinate. Thus, the radial coordinate for the starting point of the k -th electron is $\Delta r(k - 1)$. In terms of increasing emission current at constant value of $|U_{LB}|$, it seems reasonable to diminish the gap h , because the less h is, the stronger, on the average, the field is between the emitter and lens end. It can be seen in Fig. 3, *a* that even if h is essentially less than d , the equipotentials near the emitter surface bend and the field starts influencing the electrons, which are relatively low in the vicinity of the surface, like a divergent lens. If $h > 1.2d - 1.4d$ (see Fig. 3, *c*), the equipotentials bend in the opposite direction, and the field acts like a convergent lens. At $h \approx d$, the field at the surface is practically plane: it can be seen from Fig. 3, *b* that several equipotentials nearest to the emitter remain plane.

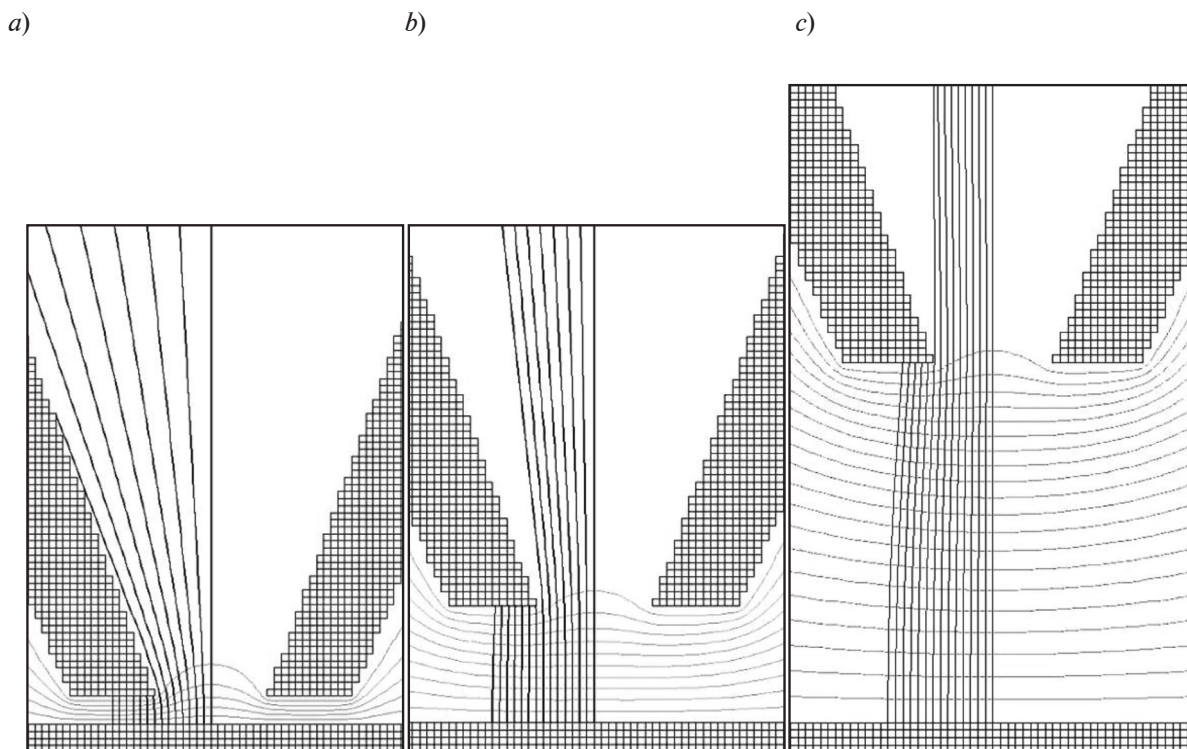


Fig. 3. Changing the pattern of the electron trajectories with the distance h , mm: 0.1 (a), 0.4(b), 1.2 (c); the lens entrance diameter $d = 0.4$ mm (see Fig. 1, b)

So, two modes can be used to study emission spectra, with the choice between these modes governed by the sample characteristics. Let us suppose that the emission centers are placed ‘densely’ on the surface: there are a lot of them in the area $S = \pi d^2 / 4$ which equals the area of the lens entrance diaphragm. Then the distance $h \approx d$ should be chosen as the minimal one at which the beam is not unfocused yet near the surface. In this situation, electrons fly in the plane field approximately half of their way towards the lens.

On the other hand, if the emission centers are placed rarely, the risk is that there are no centers opposite the diaphragm. In this case, the sample should be moved back from the diaphragm to the distance $h > 1.2d - 1.4d$, and thus the area should be enlarged of the surface useful in terms of obtaining emitted electrons. Of course, enlarging the area will be done at the sacrifice of the field strength F at the surface. The potential U_{LB} and the retarding coefficient have to be increased. It is seen in Fig. 3 that at $h = d = 0.4$ mm, eight trajectories pass through

the entrance diaphragm. This corresponds to the ‘useful’ emission area of

$$S^* = \pi[\Delta r(8 - 1)]^2 \approx 1.4 \cdot 10^5 (\mu\text{m})^2.$$

The corresponding number of trajectories is ten at $h = 3d = 1.2$ mm, and the ‘useful’ area increases:

$$S^* = \pi[\Delta r(10 - 1)]^2 \approx 2.3 \cdot 10^5 (\mu\text{m})^2.$$

After choosing relative position of the emitter and lens end, calculations were done of how to transport and focus the beam by the lens. It was again implemented with the use of the program ‘Simion7’. The following values were taken as the initial calculation parameters: three potentials of focusing electrodes U_{L1} , U_{L2} and U_{L3} , and the retarding coefficient K_{dec} , the last being defined actually by the ratio of U_{LB} to U_p . It was accepted in the calculations that $U_p = -10$ V, and that the electrons leave the emitter surface normally to it with the initial energy $E_e = 20$ meV.

Before describing the calculation results, we note that the signal was detected at the analyzer



exit by the method of single electron recording with the use of a VEU-6 secondary-electron multiplier (SEM). In the multiplier, each incoming electron produces at the exit an electron avalanche which is recorded as an electric pulse. This means that each particular electron is recorded rather than an integral electric current. The unit of signal level is ‘electrons per second’ (el/s). Using the SEM allows, on the one hand, not to worry too much about the signal intensity because an emission peak can easily be recorded even if the top intensity does not exceed 300 – 500 el/s. But on the other hand, the SEM of the model mentioned above cannot work stably if the intensity exceeds 10^5 el/s. That is why, while choosing the best focusing modes, the emphasis was made not only on the output intensity but more on minimizing the beam divergence angle at the analyzer entrance (that is at the lens exit) equal to $2\Delta\alpha$. It was accepted that $\Delta\alpha$ should not exceed two degrees. Evaluations showed that in this case the aberration blurring in the analyzer

could be neglected as the ξ value in Eq. (1) was negligible.

Fig. 4 demonstrates typical deformations of the beam axial section inside the lens and near its exit when the potentials U_{L1} , U_{L2} and U_{L3} vary. Because of the beam axial symmetry, calculations were only made for a half of its section. The source data for the results presented in the figure are as follows: $U_{LB} = +300$ V, which means, in accordance with Eq. (4), that $K_{dec} = 31$; $d = h = 0.4$ mm; the diameter of the round output lens diaphragm, which at the same time is the analyzer input one, is $d_a = 0.6$ mm. The initial electron radial coordinates are $r_i = 2(i - 1) \mu\text{m}$, where i is the ‘number’ of an electron ($i = 1, 2, \dots, N$). So, the starting point coordinate step $\Delta r = 2 \mu\text{m}$, and opposite the upper half of the lens input diaphragm

$$N = d / (2\Delta r) + 1 = 101 \text{ particles}$$

start their flights, the first one moving along the axis.

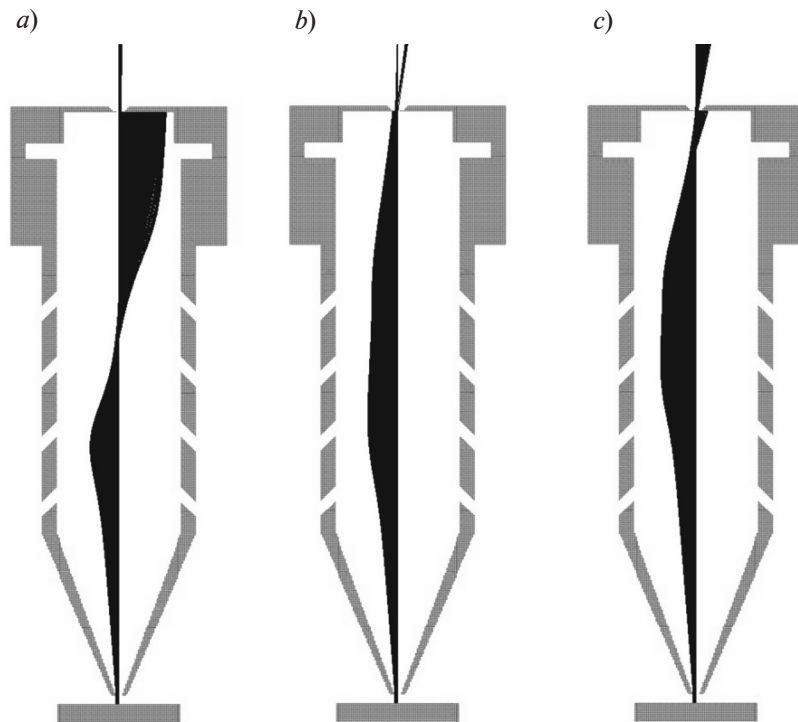


Fig. 4. Some calculated variants of the electron-beam focusing that depend on the given electrode potentials:

$U_{L1} = U_{L2} = -10$ V, $U_{L3} = 300$ V (a); $U_{L1} = U_{L2} = U_{L3} = 25$ V (b); $U_{L1} = 300$ V, $U_{L2} = U_{L3} = 30$ V (c). The rest parameters are taken constant being as follows: $U_p = 10$ V, $U_{LB} = 300$ V, $d = 0.4$ mm, $h = 0.5$ mm (see Fig. 1, b)

Fig. 4, *c* shows ‘strong’ focusing when about 50 % of the electrons whose starting points are opposite the entrance diaphragm (it means all the particles with $0 < r_i < d / 2$) pass through the exit diaphragm. These focusing conditions, nevertheless, are not appropriate, and this does not occur because the intensity can be too much for the SEM. The problem is that the divergence angle $2\Delta\alpha$ at the exit exceeds 4° , and this will cause the blurring ξ comparable with the analyzer exit slit dimension Δx_2 .

Fig. 4, *b* shows one more variant of focusing which is inappropriate for carrying out the experiment. Now, the fact of the matter is that, after passing through the diaphragm, the beam appears to be split into two weaker beams, and the angle between them lies in the range of 10 – 15 degrees. In such a case, instead of one single emission peak, two peaks or one double peak will be recorded.

In Fig. 4, *a*, the divergence angle of the beam after passing the exit diaphragm is very small, and anyway $2\Delta\alpha < 4^\circ$. The intensity of

the recorded beam I_{rec} makes approximately 4 % of the full emission current I_{full} of the electrons passing the entrance diaphragm of the lens. I_{full} was calculated as some part of the electrons passing through the lens. It is supposed meanwhile that the whole emissive area is equal to that of the entrance diaphragm. This would not be correct in the case of geometry in Figs. 3, *a* or *c*. But as d is approximately equal to h , which geometry corresponds to Fig. 3, *b*, the emitted electrons are accelerated at the early stage of their way by strong and practically plane field. This means that almost all the electrons emitted opposite the entrance diaphragm will pass it, and that almost no electrons emitted from out of this area will pass the entrance diaphragm. Thus, the relative intensity of the recorded electron flow can be evaluated as $I_{rec} / I_{full} = 4S_{em} / \pi d^2$.

Thin vertical lines in Fig. 5 show the calculated ranges of focusing corresponding to three accepted restrictions: $2\Delta\alpha < 4^\circ$; the beam at the exit is not split; $I_{rec} / I_{full} \geq 0.375$. Calculations

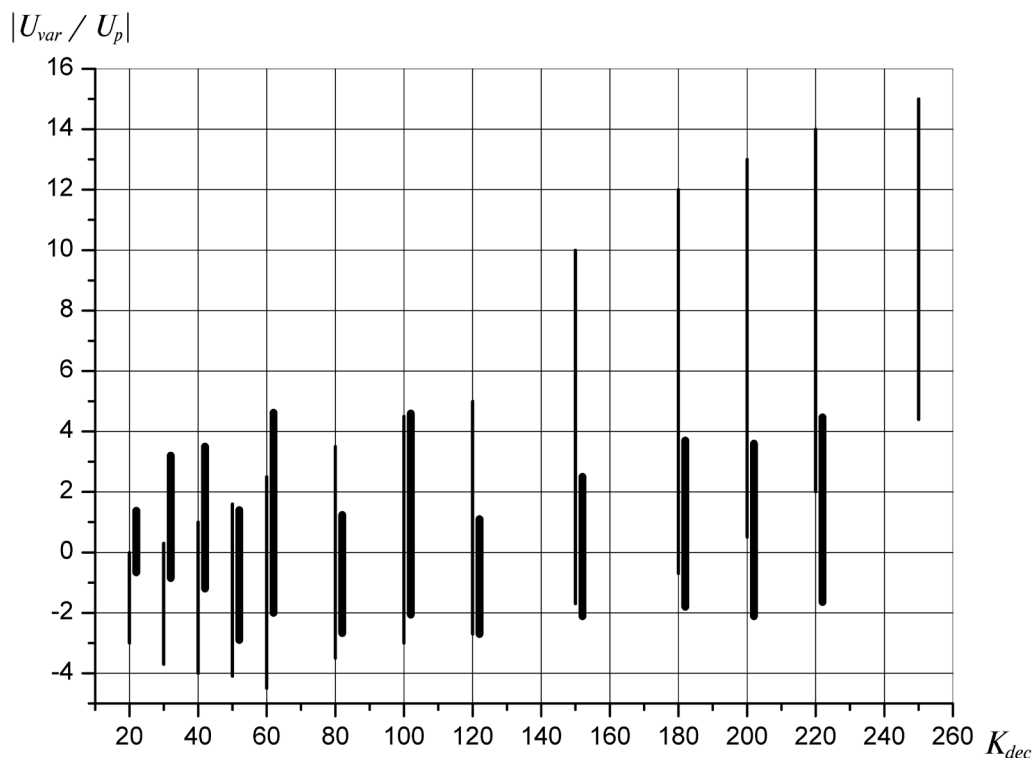


Fig. 5. The plots of the common variable potential U_{var} of the first and the second focusing electrodes ($U_{L1} = U_{L2} = U_{var}$, in terms of U_p) versus the retarding coefficient K_{dec} . The calculated (thin lines) and experimental (thick ones) ranges of focusing are presented. $2\Delta\alpha < 4^\circ$; $h = 0.7$ mm

were done under the following conditions:

the potential of the third focusing electrode was made equal to the lens body potential ($U_{L3} = U_{LB}$);

the first and the second focusing electrodes had common potential U_{var} which was varied with the idea to get the appropriate focusing of the lens. The abscissa is the retarding coefficient of the whole lens while the ordinate represents U_{var} in the units of $|U_p|$.

Under the described conditions, the bottom end of each interval of line corresponds to the beginning of the beam splitting (see Fig. 4, b). Above the top ends, $I_{rec} < 0.0375 I_{full}$. On average, for the whole range of K_{dec} , I_{rec} is more in the lower part of each interval, and the maximum of I_{rec} is as well shifted towards the lower values of $U_{var} = U_{L2} = U_{L3}$.

The focusing mode (see Fig. 5) provides a relatively high exit intensity I_{rec} . The 'saturation' of the SEM at signal levels exceeding 10^5 el/s makes it necessary (and this fact has been proved experimentally) to deliberately form relatively weak electron flows at the lens exit. One of the possible regimes of this sort has also been calculated. In this version, the first focusing electrode is electrically connected with the lens body ($U_{L1} = U_{LB}$) while the common variable potential is applied to the second and the third electrodes ($U_{var} = U_{L2} = U_{L3}$). In comparison with the previous regime, the output beam intensity is approximately 10 times less.

Even less exit intensity is achieved in the case of $U_{L1} = U_{L2} = U_{LB}$, $U_{L3} = U_{var}$. There exists, on the other hand, one more working mode possessing a bit wider intensity range. In this mode, the common ruling potential is applied to all the three focusing electrodes at once: $U_{var} = U_{L1} = U_{L2} = U_{L3}$.

Experimental test of the calculations

The tests of the calculations were carried out directly in the spectrometer vacuum chamber which had been made from 12X18H10T stainless steel, the residual gases pressure being held at the level from $7 \cdot 10^{-6}$ to $4 \cdot 10^{-5}$ Pa. To minimize the harmful influence from any strain magnetic fields including that of the Earth on the experiment, the spectrometer was placed inside Helmholtz coils. The measure-

ments, which were carried out while the proper Helmholtz coil currents were being chosen, proved that the residual magnetic induction B did not exceed $40 \mu\text{T}$ in the spectrometer volume, while B did not exceed $20 \mu\text{T}$ in the area of the top part of the electron trajectory inside the analyzer. The last fact is particularly important because the electron kinetic energy is minimal just in the mentioned area. Thus, the Earth's magnetic field, which is around $50 \mu\text{T}$ in Saint Petersburg, was reduced by a factor of $125 - 250$.

A flat indirectly heated thermoemitter of reduced work function was used as a test unit. In case it was necessary to increase the emission level, an activation procedure was provided by means of heating the sample at approximately $800 \text{ }^\circ\text{C}$ and simultaneously taking the emission current. Out of the activation process, the working emitter temperature was held at the level of $600 \leq T_e \leq 800 \text{ }^\circ\text{C}$.

The experiment was carried out at the following geometric parameters (see Fig. 1, b): $h \approx 0.6 - 0.8 \text{ mm}$; $d = 0.4 \text{ mm}$; $G = 1.0 \text{ mm}$. It was difficult to determine accurately the value h for two reasons:

- (i) it was undesirable to touch emitting surface with a feeler;
- (ii) the cathode could have been deformed a little during its heating.

The input analyzer diaphragm was round of the diameter $d_a = 0.6 \text{ mm}$, so Δx_1 in formulae (1) can be taken as 0.6 mm . The width of the rectangular slit in the analyzer output $\Delta x_2 = 0.2 \text{ mm}$.

Thus, the resolving power R_{sp} of the whole spectrometer can easily be calculated. If E_{sp} is the electron energy at the lens entrance diaphragm

$$(E_{sp} = |(U_{LB} - U_p) e|),$$

then, in the case that the aberrational blurring ξ of the analyzer is negligible,

$$\begin{aligned} R_{sp} &= \frac{E_{sp}}{\Delta E} = \frac{|(U_{LB} - U_p) e|}{\Delta E} = \\ &= \frac{K_{dec} \cdot E_p}{\Delta E} = K_{dec} \cdot D \cdot \frac{X}{\Delta x_1 + \Delta x_2}. \end{aligned} \quad (5)$$

If, for example, $K_{dec} = 120$, then, in accordance with Eq. (5), $R_{sp} = 9 \cdot 10^4$ which means

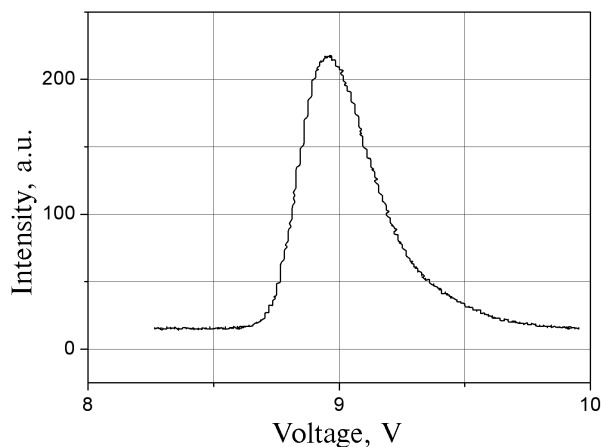


Fig. 6. A typical thermoemission spectrum which was taken from the initially cleaned emitter

that the calculated base resolving power exceeds the minimal required value by the factor of 4.5. Actually, if the geometric factors Δx_1 and Δx_2 are fixed, then ΔE only depends on E_p , and the K_{dec} value only specifies the voltage that should be applied to the lens entrance to elicit electrons from the emitter. For instance, at $E_p = 10$ eV, the absolute resolution ΔE of the spectrometer should be equal to 13.3 meV, no matter the value of U_{LB} .

Fig. 6 demonstrates a typical thermoemission spectrum measured from the sample under study (it had initially been well-cleaned by heating). Here, the abscissa V is the energy of the recorded electrons divided by the electron charge. The peak was recorded at $E_p = 9$ eV and $K_{dec} = 120$. It is asymmetric, the shape being determined by the Maxwell – Boltzmann distribution at the particular emitter temperature (approximately 700 K). Its FWHM is 335 meV, its left edge corresponds to the lowest emitted electrons while the right-hand part arises from the ‘tail’ of the distribution. The width of the left front is $\Delta E_{lf} \approx 130 - 150$ meV, which corresponds to the spatial distribution of the electrons at the surface at $T = 700$ K. The maximal peak intensity at the top is 22,000 el/s.

Recording peaks similar to the one described above gave rise to the general picture of typical operating parameters of the spectrometer that were acceptable for studying the emission spectra. As a comparison with the calculated parameters, thick lines in Fig. 5 show

the experimentally obtained focusing ranges. At any particular K_{dec} , the main criteria of whether a value $U_{var} = U_{L1} = U_{L2}$ was acceptable for spectra recording was the intensity of the peak, its shape staying unvaried. At the boundaries of each range, the intensity is half of its maximum. Because of the relatively high FWHM, peak splitting was not always observed but if it was, the corresponding part of the range was cut off. It can be seen in Fig. 5 that experimental data only partly overlap the theoretical one. One of the reasons for this is the difference in the corresponding criteria. Besides, stray fields, including the magnetic one produced by the heater, and stray electrostatic fields arising from the inhomogeneity of the analyzer and lens surfaces, could add their contributions as well. Nevertheless, the conclusion can be made up that it is possible to record the spectra of field-induced emission under the conditions which satisfy both experimentally and theoretically deduced criteria. Under these conditions, a narrow peak of field emission (it is expected to be narrow in comparison with the thermoemission peak) should not appear double, and at the same time it is supposed to be rather intensive. For instance, in the mode of Fig. 5, if $K_{dec} = 120$, then the common potential of the first and second lens electrodes can be varied from approximately $-2.5|U_p|$ to some $+0.5|U_p|$. If $K_{dec} = 220$, then the experimental and theoretical results overlap in the region

$$2|U_p| < U_{var} = U_{L1} = U_{L2} < 4.5|U_p|.$$

If, before spectra recording, the emitter had not been properly heated and as a result it had not been carefully cleaned from adsorbed impurities, the emission spectra were observed whose shapes were either a peak with a ‘shoulder’ or a double and even a triple peak. The fact that the peak splitting did not come from electron-optical conditions could easily be verified by just changing these conditions. Fig. 7 demonstrates how the shape of a spectrum changed with U_{LB} increasing. Increasing U_{LB} means, first of all, the growth of the field strength F on the emitter surface. At a relatively small F value, a single ‘shouldered’ peak was recorded, the shoulder being placed at the high-energy side, with the whole FWHM of approximately 1 eV (Fig. 7, curve 1 where

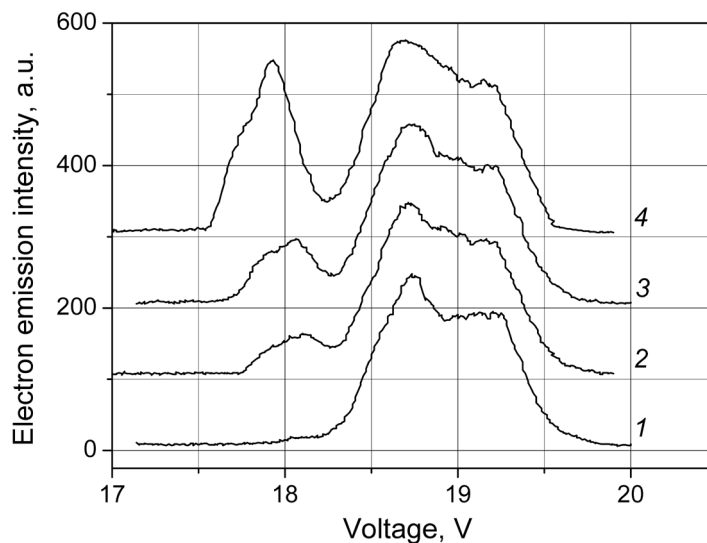


Fig. 7. Emission spectra changing with an increase in the field strength F , V/mm: ≈ 1170 (1), ≈ 1740 (2), ≈ 2300 (3), ≈ 2600 (4); the field strength was estimated near the emitter surface

$F \approx 1170$ V/mm). There can only be noticed a miniscule shoulder at the low-energy side. As the field strength grew (curve 2 where $F \approx 1740$ V/mm and 3 with $F \approx 2300$ V/mm in Fig. 7), the weak shoulder transformed to a noticeable peak, the FWHM of the rest of the spectrum staying practically unchanged. Finally, this low-energy peak became almost equal in intensity to the main shouldered peak (curve 4 where $F \approx 2600$ V/mm in Fig. 7). The whole energy range of the spectrum became equal to 2 eV with the distance between the two tops of approximately 700 meV.

The aim of this work was not to study thoroughly thermo- or field-emission of a multicomponent sample. That is why careful analysis of the reasons for spectra changing with F was not done. It should be noticed that the shape of the spectra changed rather significantly not only with F but when the sample temperature was varied, too. The spectrometric results shown here are only to demonstrate that the spectra recorded with the use of the novel spectrometer can reflect the dynamical processes taking place on the surface of a plane emitter.

Summary

A novel electron spectrometer has been made to study the low-voltage field emission

from the surfaces of nanostructured objects such as nanoporous carbon, carbon nanotubes, nanocarbon films and other carbon structures. Calculations showed that the resolving power of the apparatus could easily achieve the values of the order of 10^5 , the absolute energy resolution being of the order of 10 meV. This data was obtained through using a non-traditional high-dispersion energy analyzer with the enhanced dispersion $D \approx 12-13$, and a retarding lens system with the retarding coefficient variable in the wide range, up to 250 and more.

The working modes of the spectrometer were tested experimentally with the use of a thermoemitter as a sample. All the abilities of the new spectrometer cannot, of course, be proved while recording thermoemission spectra, because the last do not possess sharp singularities of about 10 meV in width. Nevertheless, emission peaks were recorded just in the calculated modes, and the physical phenomena taking place on the emitter surface were demonstrated to be reflected in the form of the recorded spectra.

Three working modes of the spectrometer have been revealed which are meant for strongly different levels of recorded signals. The minimal emission current at which spectra recording is possible is evaluated to be about 0.1 nA.

REFERENCES

- [1] V.B. Bondarenko, P.G. Gabdullin, N.M. Gnuchev, et al., Emissivity of powders prepared from nanoporous carbon, *Technical Physics*. 49 (10) (2004) 1360–1363.
- [2] A.A. Arkhipov, S.N. Davydov, P.G. Gabdullin, et al., Field-induced electron emission from nanoporous carbons, *Journal of Nanomaterials*. 2014 (2014) ID 190232, 9 p.
- [3] A.V. Elelskii, Carbonnanotube-based electron field emitters, *Phys. Usp.* 53(9) (2010) 863–892.
- [4] D.J. Jarvis, H.L. Andrews, C.L. Ivanov, et al., Resonant tunneling and extreme brightness from diamond field emitters and carbon nanotubes, *J. Appl. Phys.* 108(9) (2010) 094322.
- [5] S.Yu. Suzdal'tsev, V.Ya. Shanygin, R.K. Yafarov, Field-emission diode with tangential current take off from thin-film nanodiamond/graphite emitter, *Technical Physics Letters*. 37(6) (2011) 534–537.
- [6] S. Pandey, P. Rai, S. Patole, et al., Improved electron field emission from morphologically disordered monolayer graphene, *Appl. Phys. Lett.* 100 (4) (2012) 043104.
- [7] I.G. Kozlov, *Sovremennyye problemy elektronnoy spektroskopii* [Present-day problems of spectroscopy], Moscow, Atomizdat, 1978.
- [8] Yu.K. Golikov, S.N. Davydov, V.V. Korablev, *Elektronnyy spektrometr s monokhromatizatsiyey zondiruyushchego potoka i uvelichennoy ploshchady skanirovaniya obraztsa* [Electronic spectrometer with monochromatization of sounding flow and magnified area of sample scanning], *Pribery i tehnika eksperimenta*. No. 4 (1991) 143–148.
- [9] Yu.A. Kudinov, S.I. Fedoseenko, S.N. Davydov, et al., Measuring the energy distribution of slow photoelectrons with a high-dispersion analyzer, *Institution of Engineering and Technology*. 36 (4) (1993) 608–610.
- [10] S.N. Davydov, Yu.A. Kudinov, Yu.K. Golikov, et al., High-resolution electron energy analyser for angle-resolved spectroscopy, *J. Electron Spectrosc. Relat. Phenom.* 72 (1995) 317–321.
- [11] Yu.K. Golikov, V.V. Korablev, S.N. Davydov, et al., Non-traditional systems of charged particle optics for electron spectroscopy and mass spectrometry, *Proc. of SPIE*. 4064 (2000) 58–79.
- [12] S.N. Davydov, P.G. Gabdullin, M.A. Ryumin, Apparatus for investigating physical nature of nanoporous carbon structure field emission, *Book of abstracts, 9-th Biennial International workshop "Fullerenes and Atomic Clusters"*. July 6-10 (2009) SPb, Russia, P.165.
- [13] S.N. Davydov, Electrostatic systems of monochromatization and energy analysis of electron flows, Ph. D. thesis, Leningrad Polytechnic Institute, 1989.

THE AUTHORS

BONDARENKO Vyacheslav B.

Peter the Great St. Petersburg Polytechnic University
29 Politechnicheskaya St., St. Petersburg, 195251, Russian Federation
phys-el@spbstu.ru

DAVYDOV Sergey N.

Peter the Great St. Petersburg Polytechnic University
29 Politechnicheskaya St., St. Petersburg, 195251, Russian Federation
Wearehappy2008@yandex.ru

GABDULLIN Pavel G.

Peter the Great St. Petersburg Polytechnic University
29 Politechnicheskaya St., St. Petersburg, 195251, Russian Federation
pavel-gabdullin@yandex.ru

GNUCHEV Nikolay M.

Peter the Great St. Petersburg Polytechnic University
29 Politechnicheskaya St., St. Petersburg, 195251, Russian Federation
gnuchev.nm@spbstu.ru

MASLEVTSOV Andrey V.

Peter the Great St. Petersburg Polytechnic University
29 Politechnicheskaya St., St. Petersburg, 195251, Russian Federation
phys-el@spbstu.ru

ARKHIPOV Anton A.

Peter the Great St. Petersburg Polytechnic University

29 Politechnicheskaya St., St. Petersburg, 195251, Russian Federation

zuarhipanton@mail.ru

Бондаренко В.Б., Давыдов С.Н., Габдуллин П.Г., Гнучев Н.М., Маслецов А.В., Архипов А.А. ЭЛЕКТРОННЫЙ СПЕКТРОМЕТР ДЛЯ ИССЛЕДОВАНИЯ ПОЛЕВОЙ ЭМИССИИ НАНОСТРУКТУР.

Создан новый электронный спектрометр для исследования низкополевой эмиссии наноструктурированных объектов, в частности нанопористого углерода, нанотрубок и других углеродных структур. Высокая расчетная разрешающая способность прибора получена, в основном, за счет применения оригинального энергоанализатора с высокой дисперсией и замедления анализируемого потока электронов в десятки и сотни раз по энергии. Режимы работы спектрометра опробованы на эксперименте с использованием термоэмиттера в качестве тестового образца. В работе продемонстрировано также, что физические явления, происходящие на поверхности эмиттера, отражаются на виде регистрируемого спектра. Выявлено три режима работы прибора, рассчитанных на уровни эмиссии, отличающиеся друг от друга приблизительно на порядок. Минимальный ток эмиссии, при котором возможна регистрация спектра, составляет примерно 0,1 нА.

НИЗКОВОЛЬТНАЯ ПОЛЕВАЯ ЭМИССИЯ, АВТОЭМИССИЯ, ПОЛЕВАЯ ЭМИССИЯ НАНОСТРУКТУР, ВЫСОКАЯ РАЗРЕШАЮЩАЯ СПОСОБНОСТЬ.

СПИСОК ЛИТЕРАТУРЫ

- [1] **Бондаренко В.Б., Габдуллин П.Г., Гнучев Н.М. и др.** Эмиссионные характеристики порошков из нанопористого углерода // *ЖТФ*. 2004. Т. 74. Вып. 10. С. 113–116.
- [2] **Arkhipov A., Davydov S.N., Gabdullin P.G., et al.** Field-induced electron emission from nanoporous carbons // *Journal of Nanomaterials*. 2014. Vol. 2014. Article ID 190232. 9 p.
- [3] **Елецкий А.В.** Холодные полевые эмиттеры на основе углеродных нанотрубок // *УФН*. 2010. Т. 180. Вып. 9. С. 897–930.
- [4] **Jarvis D.J., Andrews H.L., Ivanov, C.L. et al.** Resonant tunneling and extreme brightness from diamond field emitters and carbon nanotubes // *J. Appl. Phys.* 2010. Vol. 108. No. 9. P. 094322.
- [5] **Суздальцев С.Ю., Шаныгин В.Я., Яфarov P.K.** Исследование автоэмиссионного диода с тангенциальным токоотбором из тонкоплечного наноалмазографитового эмиттера // *Письма в ЖТФ*. 2011. Т. 37. Вып. 11. С. 91–98.
- [6] **Pandey S., Rai P., Patole S., et al.** Improved electron field emission from morphologically disordered monolayer grapheme // *Appl. Phys. Lett.* 2012. Vol. 100. No. 4. P. 043104.
- [7] **Козлов И.Г.** Современные проблемы электронной спектроскопии. М.: Атомиздат, 1978, 248 с.
- [8] **Голиков Ю.А., Давыдов С.Н., Кораблев В.В.** Электронный спектрометр с монохроматизацией зондирующего потока и увеличенной площадью сканирования образца // *Приборы и техника эксперимента*. 1991. № 4. С. 143–148.
- [9] **Kudinov Yu.A., Fedoseenko S.I., Davydov S.N., et al.** Measuring the energy distribution of slow photoelectrons with a high-dispersion analyzer // *Institution of Engineering and Technology*. 1993. Vol. 36. No. 4. Pp. 608–610.
- [10] **Davydov S.N., Kudinov Yu.A., Golikov Yu.K., et al.** High-resolution electron energy analyser for angle-resolved spectroscopy // *J. Electron Spectrosc. Relat. Phenom.* 1995. Vol. 72. Pp. 317–321.
- [11] **Golikov Yu.K., Korablev V.V., Davydov S.N., et al.** Non-traditional systems of charged particle optics for electron spectroscopy and mass spectrometry // *Proceedings of SPIE*. 2000. Vol. 4064. Pp. 58–79.
- [12] **Davydov S.N., Gabdullin P.G., Ryumin M.A.** Apparatus for investigating physical nature of nanoporous carbon structure field emission // *Book of abstracts. 9-th Biennial International workshop “Fullerenes and Atomic Clusters”*. July 6-10, 2009. SPb, Russia. P. 165.
- [13] **Давыдов С.Н.** Электростатические системы монохроматизации и анализ энергии электронных потоков. Дис. канд. физ.-мат. наук. Ленинград: ЛПИ им. М.И. Калинина, 1989.

СВЕДЕНИЯ ОБ АВТОРАХ

БОНДАРЕНКО Вячеслав Борисович – кандидат физико-математических наук, доцент кафедры физической электроники Санкт-Петербургского политехнического университета Петра Великого.

195251, Российская Федерация, г. Санкт-Петербург, Политехническая ул., 29
phys-el@spbstu.ru

ДАВЫДОВ Сергей Николаевич – кандидат физико-математических наук, доцент кафедры физической электроники Санкт-Петербургского политехнического университета Петра Великого.

195251, Российская Федерация, г. Санкт-Петербург, Политехническая ул., 29
Wearehappy2008@yandex.ru

ГАБДУЛЛИН Павел Гарифович – кандидат физико-математических наук, доцент кафедры физической электроники Санкт-Петербургского политехнического университета Петра Великого.

195251, Российская Федерация, г. Санкт-Петербург, Политехническая ул., 29
pavel-gabdullin@yandex.ru

ГНУЧЕВ Николай Михайлович – доктор физико-математических наук, профессор кафедры физической электроники Санкт-Петербургского политехнического университета Петра Великого.

195251, Российская Федерация, г. Санкт-Петербург, Политехническая ул., 29
gnuchev.nm@spbstu.ru

МАСЛЕВЦОВ Андрей Вадимович – заведующий лабораторией кафедры физической электроники Санкт-Петербургского политехнического университета Петра Великого.

195251, Российская Федерация, г. Санкт-Петербург, Политехническая ул., 29
phys-el@spbstu.ru

АРХИПОВ Антон Андреевич – студент Института прикладной математики и механики Санкт-Петербургского политехнического университета Петра Великого.

195251, Российская Федерация, г. Санкт-Петербург, Политехническая ул., 29
zuarhipanton@mail.ru